

# CMOS Phase-Locked-Loop Applications Using the CD54/74HC/HCT4046A and CD54/74HC/HCT7046A

by W.M.Austin

This Application Note provides the circuit designer with information on the use of the CD54/74HC/HCT4046A Phase-Locked Loop (PLL) with voltage-controlled oscillator (VCO) and the CD54/74HC/HCT7046A Phase-Locked Loop with In-Lock Detection in phase-locked circuits. A description of the basic loop operation is included as an introduction to phase-lock techniques. In the description, the CMOS PLL IC provides the phase comparators, VCO, VCO inhibit, plus the lock detectors and indicators for the loop. Complete circuit designs with and without a frequency-divide ratio are included as examples. Examples are also given of various filters operating over a range of frequencies.

## BASIC LOOP OPERATION

The CD54/74HC/HCT4046A Phase-Locked Loop (PLL) with voltage-controlled oscillator (VCO) is a High-Speed CMOS IC designed for use in general-purpose PLL applications including frequency modulation, demodulation, discrimination, synthesis, and multiplication. Specific applications include data synchronizing, conditioning and tone decoding, as well as direct VCO use for voltage-to-frequency conversion and speed-control applications.

The IC contains a VCO and a choice of phase comparators (PCs) for support of the basic PLL circuit, as shown in Fig. 1(a). The low-pass filter (LPF) is an essential part of the loop and is needed to suppress noise and high-frequency components. An optional fourth part of the loop is the divide-by-N frequency divider, which is needed when the VCO is run at a multiple of the signal-input reference frequency. To facilitate support of a variety of general-purpose applications, both the filter and divider are external to the HC/HCT4046A. These and other aspects of the application of the HC/HCT4046A are explained below through a variety of loop design examples.

For a full treatment of PLL theory, the reader is directed to the bibliography where there are a number of references that support the descriptions and explanations given below. The symbols and terminology used in this Note primarily follow the book, *Phase-Lock Techniques*, by Gardner.<sup>1</sup> The details of derivations of the equations can be found in the references.

Some understanding of feedback theory as a background for designing PLL circuits is helpful, but lack of this understanding should not be a deterrent to anyone choosing

to apply the HCHCT4046A in relatively simple, second-order PLL circuits. The purpose of the Note is to present a solid tutorial on CMOS PLL techniques, including extensive information on the VCO characteristics. A designer can then apply the information to a variety of circuit applications.

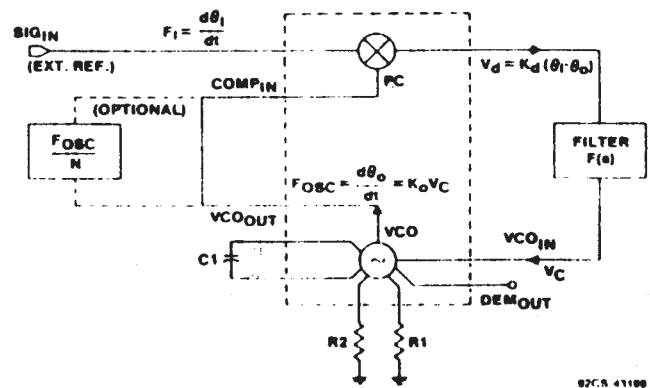


Fig. 1(a) - Block diagram of an HC/HCT4046A in a typical phase-locked-loop circuit.

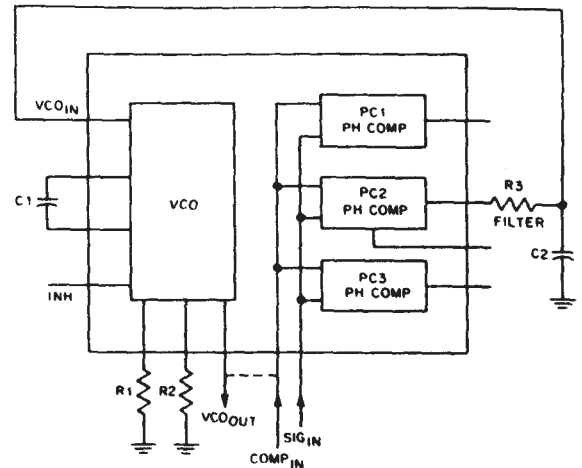
Before beginning to apply the HC/HCT4046A in PLL circuits, a designer should have an understanding of the parameters and equations used to define loop performance. Further, the designer should recognize that PLL circuits are a special case of feedback systems. Where servomechanism feedback systems are primarily concerned with position control, PLL feedback systems are primarily concerned with the phase and tracking of a VCO relative to a reference signal input. While a phase error can be anticipated, no differential in frequency is desired after phase-lock is established. General feedback theory is applied in PLL use just as it is in servomechanism systems. Some of the symbols and terminology used to describe PLL systems were borrowed from servo systems, giving rise to such terms as damping factor, natural loop resonant frequency, and loop bandwidth.



## DESCRIPTION OF THE HC/HCT4046A

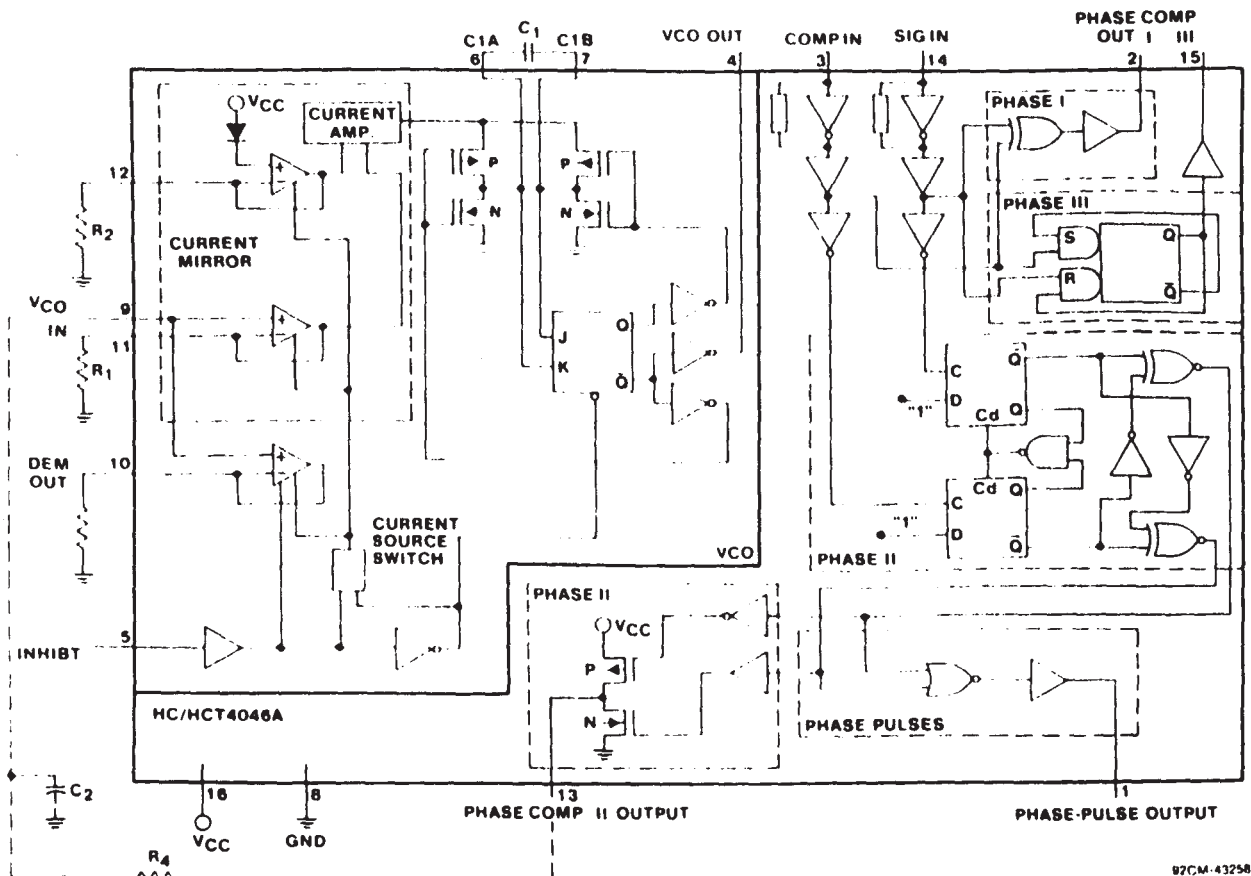
The block diagram of the HC/HCT4046A, Fig. 1(b), illustrates the least complex form of external loop filtering. In addition to the VCO, the HC/HCT4046A provides a choice of three phase comparators. The HC/HCT7046A is an equivalent device, differing only in the trade-off of a third phase comparator (PC3) for a lock detector (LD). The pinouts of the HC/HCT4046A and HC/HCT7046A differ in a minor way from that of the earlier CMOS PLL-type CD4046B, which differs functionally in that it has a zener reference diode in place of PC3 or the lock detector. Unless otherwise noted in the following information, all description and operational references apply to both the HC/HCT4046A and HC/HCT7046A.

Figs. 2(a) and 2(b) show the HC/HCT4046A and HC/HCT7046A functional block diagrams, respectively. The VCO of the HC/HCT4046A is identical to that of the HC/HCT7046A and has the same operating characteristics. The HCT versions of these oscillator circuits differ from the HC versions by having TTL logic levels at the inhibit inputs. Improved linear differential amplifiers are used to control the current bias established by resistors  $R_1$  and  $R_2$ ; amplifying current mirrors control the charge rate of the timing capacitor  $C_1$ . Descriptive and design information on frequency control of the VCO is given below.



92CS-43156

Fig. 1(b) - Block diagram of an HC/HCT4046A illustrating external loop filtering.



97CM-43258

Fig. 2(a) - Functional block diagram of HC/HCT4046A.

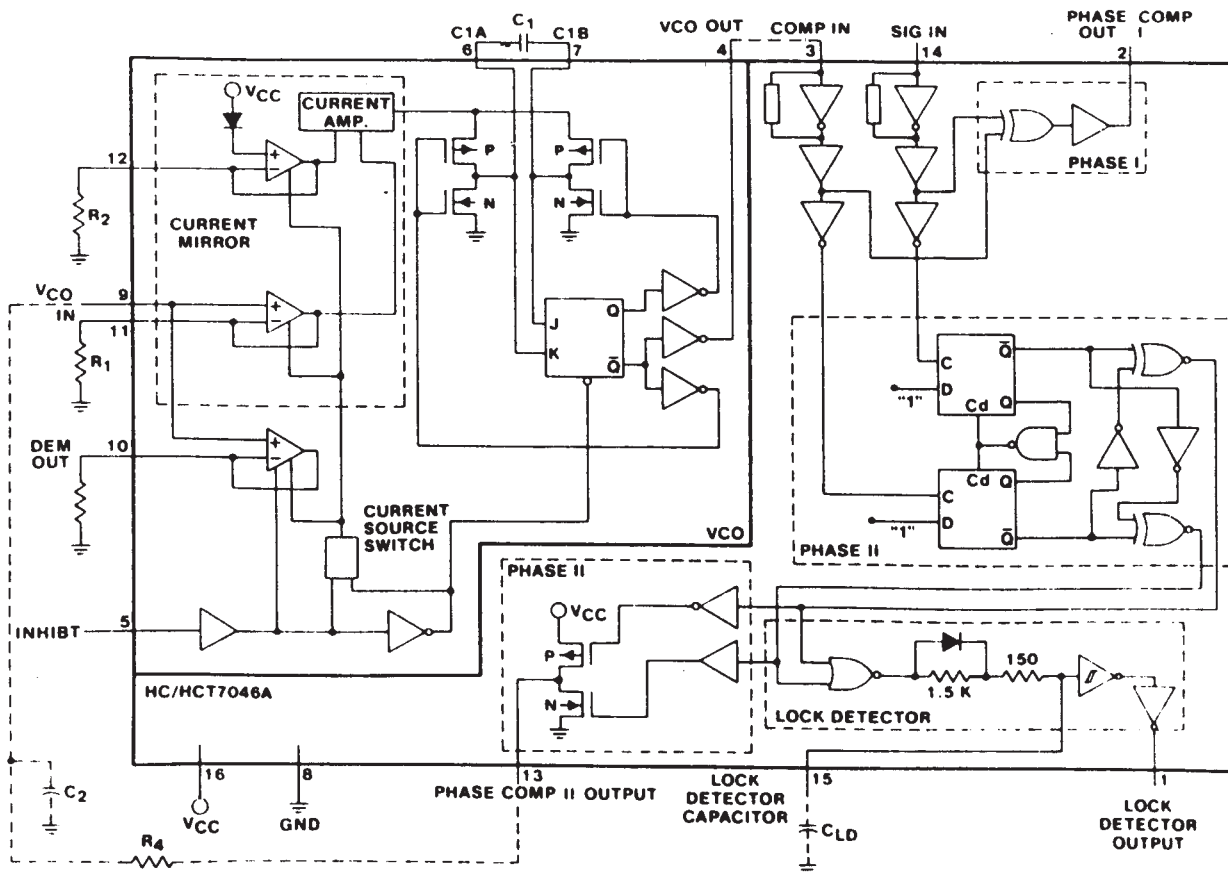


Fig. 2(b) - Functional block diagram of HC/HCT7046A.

## PHASE COMPARATORS

While there are many types of phase comparators (PCs -also referred to as detectors), the ones chosen for the CMOS PLL design are based on accepted industry-standard types. The choice was also based on design flexibility and the compatibility of CMOS technology with PC applications. Fig. 2(a) shows the logic diagram of the phase-comparator circuit with PC1, PC2, and PC3 identified. The comparators consist of an Exclusive-OR (PC1), an edge-triggered JK flip-flop (PC2), and an edge-triggered RS flip-flop (PC3). The phase comparator inputs are in parallel, making the user's choice a matter of selecting the pinout to the preferred PC.

Both the external-reference signal input and the comparator input are internally self-biased to  $V_{DD}/2$  to permit ac coupling from the drive signal sources. When ac-coupled input signals are used, the drive sensitivity is typically better than 50 mV<sub>pp</sub>. The comparator input is normally used for the VCO direct-coupled input; however, the comparator section is independent of the VCO for stand-alone use.

The signals to both phase-comparator inputs are amplified with limiting that ignores amplitude changes. With respect to the HC4046A versus the HCT4046A, only the inhibit input

levels are different; the drive levels for the phase comparator inputs are the same. When TTL drive levels are used for the signal input to the detectors, either ac coupling or TTL-to-CMOS level conversion should be used to correctly drive the  $V_{DD}/2$  switch level. Where the signal-input source voltage is less than the logic level in peak-to-peak amplitude, ac coupling is necessary. In addition, ac coupling is preferred with reduced drive signals to minimize transient switching and harmonic interference with the VCO.

Appendix I provides a summary of the phase-comparator options. An extended description of the three phase comparators follows.

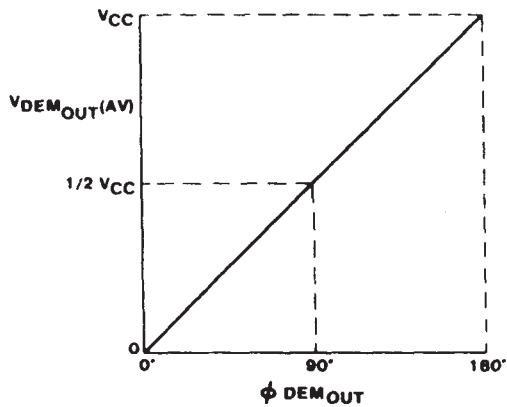
### Operation of Phase Comparator PC1

PC1 is an Exclusive-OR logic circuit. The signal and comparator input frequencies ( $f_i$ ) must have a 50% duty factor for the maximum locking range to be obtained. The transfer characteristic of PC1, assuming the ripple frequency ( $f_r = 2f_i$ ) is suppressed, is:

$$V_{DEMout} = (V_{CC}/\pi)(\phi_{SIGin} - \phi_{COMPin}) = V_{PC1out}$$

where  $V_{DEMout}$  is the demodulator output at pin 10 and equals  $V_{PC1out}$  via the low-pass filter (LPF).  $\phi$  is the phase angle in degrees.

The average output voltage from PC1, fed to the VCO input via the LPF and seen at the demodulator output at pin 10, is the resultant of the phase differences of signals ( $SIG_{in}$ ) and the comparator input ( $COMP_{in}$ ), as shown in Fig. 3(a). The average of  $V_{DEMout}$  is equal to  $V_{CC}/2$  when there is no signal or noise at  $SIG_{in}$ , and with this input the VCO oscillates at the center frequency ( $f_0$ ). Typical waveforms for the PC1 loop locked at  $f_0$  are shown in Fig. 3(b).

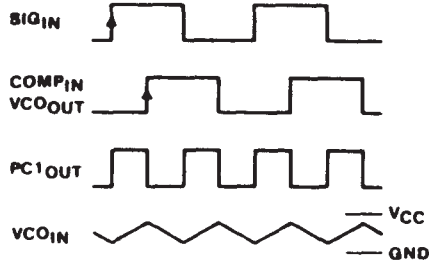


92CS-43200

Fig. 3(a) - Phase comparator PC1 average output voltage as a function of input phase difference.

$$V_{DEMout} = V_{PC1out} = (V_{CC}/\pi)(\phi_{SIGin} - \phi_{COMPin})$$

$$\phi_{DEMout} = (\phi_{SIGin} - \phi_{COMPin})$$



92CS-43203

Fig. 3(b) - Typical waveforms for PLL using phase comparator PC1 loop locked at  $f_0$ .

The frequency-capture range ( $2f_c$ ) is defined as the frequency range of input signals on which the PLL will lock for initially out-of-lock conditions. The frequency lock range ( $2f_l$ ) is defined as the frequency range of input signals on which the locked loop will remain in lock. The capture range is smaller or equal to the lock range. The capture range of PC1 depends on the LPF characteristics and can be made as large as the lock range. This configuration retains lock behavior even with very noisy signal input. PC1 can lock to input frequencies within the locking range of VCO harmonics.

### Operation of Phase Comparator PC2

For most applications, the features of PC2 provide the most advantages. It is a positive-edge-triggered phase and frequency detector. When the PLL uses this comparator, the loop is controlled by positive signal transitions, and control of the duty factor of  $SIG_{in}$  and  $COMP_{in}$  is not required. PC2 is composed of two D-type flip-flops and a 3-state output stage and has controlled-gating. The circuit functions as an up-down counter, where  $SIG_{in}$  causes an up count and  $COMP_{in}$  a down count. The transfer function of PC2, assuming ripple ( $f_r = f_i$ ) is suppressed, is:

$$V_{DEMout} = (V_{CC}/4\pi)(\phi_{SIGin} - \phi_{COMPin}) = V_{PC2out}$$

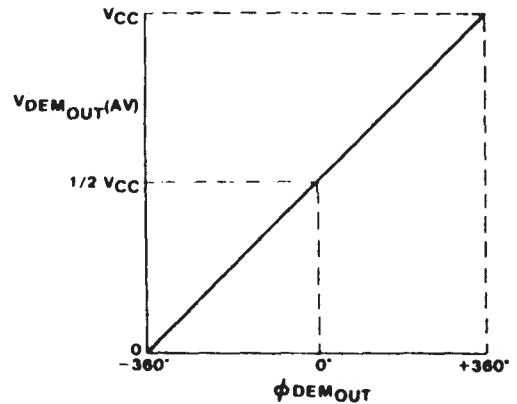
OR

$$V_{DEMout} = (V_{CC}/2\pi)(\phi_{SIGin} - \phi_{COMPin}) = V_{PC2out}^*$$

where the PC2 gain is mode dependent.

\*(Refer to Appendix II.)

The average output voltage from PC2, fed to the VCO via the LPF and seen at the demodulator output at pin 10, is the resultant of the phase differences of  $SIG_{in}$  and  $COMP_{in}$ , as shown in Fig. 4(a). Typical waveforms for the PC2 loop locked at  $f_0$  are shown in Fig. 4(b).

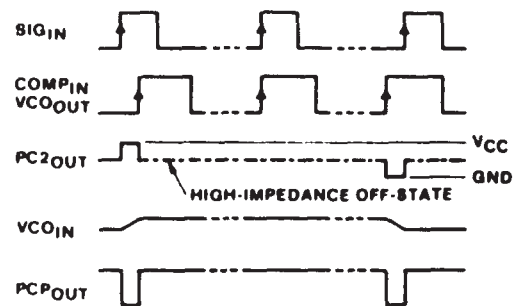


92CS-43201

Fig. 4(a) - Phase comparator PC2 average output voltage as a function of input phase difference.

$$V_{DEMout} = V_{PC2out} = (V_{CC}/4\pi)(\phi_{SIGin} - \phi_{COMPin})$$

$$\phi_{DEMout} = (\phi_{SIGin} - \phi_{COMPin})$$



92CS-43204

Fig. 4(b) - Typical waveforms for PLL using phase comparator PC2 loop locked at  $f_0$ .



When the frequencies of SIG<sub>in</sub> and COMP<sub>in</sub> are equal, but the phase of SIG<sub>in</sub> leads that of COMP<sub>in</sub>, the PMOS device at the PC2 output (Fig. 2) is held on for a time corresponding to the phase difference. When the phase of SIG<sub>in</sub> lags that of COMP<sub>in</sub>, the NMOS device is held on. When the frequency of SIG<sub>in</sub> is higher than that of COMP<sub>in</sub>, the PMOS device is held on for a greater portion of the signal cycle time. For most of the remainder of the cycle time, the NMOS and PMOS devices are off (3-state). If the SIG<sub>in</sub> frequency is lower than the COMP<sub>in</sub> frequency, then it is the NMOS device that is held on for most of the cycle.

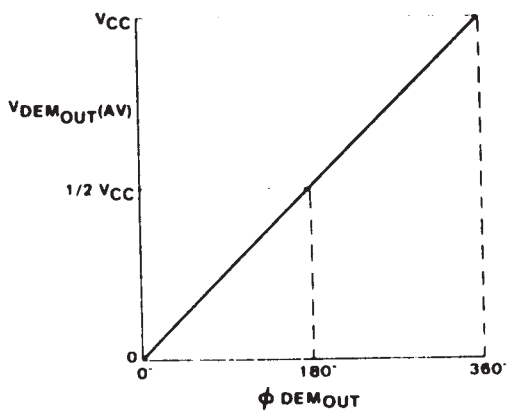
As locked conditions are achieved, the filtered output voltage from PC2 corrects the VCO until the comparator input signals are phase locked. Under stable phase-locked conditions, the VCO input voltage from the output of the LPF is constant, and the PC2 output is in a 3-state condition.

#### Operation of Phase Comparator PC3 (HC/HCT4046A Only)

The circuit of PC3 is a positive-edge-triggered sequential phase detector that uses an RS flip-flop. When PC3 is used as the PLL phase comparator, the loop is controlled by positive signal transitions. This type of detector is not sensitive to the duty factor of SIG<sub>in</sub> and COMP<sub>in</sub>. The transfer characteristic of PC3, assuming ripple (f<sub>r</sub> = f<sub>i</sub>) is suppressed, is:

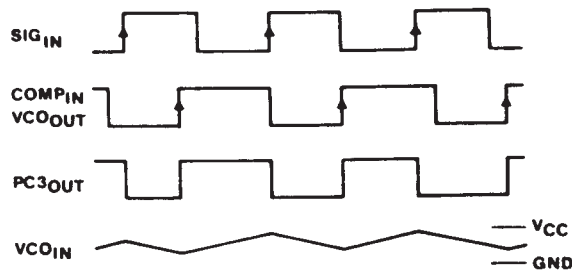
$$V_{\text{DEMOUT}} = (V_{\text{CC}}/2\pi)(\phi_{\text{SIGin}} - \phi_{\text{COMPin}}) \\ = V_{\text{PC3out}} \text{ via the LPF}$$

The average output from PC3, fed to the VCO via the LPF and seen at the demodulator output, is the resultant of the phase differences of SIG<sub>in</sub> and COMP<sub>in</sub>, as shown in Fig. 5(a). The typical waveforms for the PC3 loop locked at f<sub>o</sub> are shown in Fig. 5(b).



5(a) - Phase comparator PC3 average output voltage as a function of input phase difference.

$$V_{\text{DEMOUT}} = V_{\text{PC3out}} = (V_{\text{CC}}/2\pi)(\phi_{\text{SIGin}} - \phi_{\text{COMPin}}) \\ \phi_{\text{DEMOUT}} = (\phi_{\text{SIGin}} - \phi_{\text{COMPin}})$$



92CS-43205

Fig. 5(b) - Typical waveforms for PLL using phase comparator PC3 loop locked at f<sub>o</sub>.

The phase characteristics of PC3 differ from those of PC2 in that the phase angle between SIG<sub>in</sub> and COMP<sub>in</sub> in PC3 varies between zero and 360 degrees, and is 180 degrees at the center frequency. PC3 also has a greater voltage swing than PC2 for the same input phase differences. While the conversion gain may be higher in PC2, PC3 produces a higher ripple content in the VCO or COMP<sub>in</sub> signal.

#### LOCK INDICATORS

##### PCP<sub>out</sub> of the HC/HCT4046A

Although the phase-comparator pulse output (PCP<sub>out</sub>) is shown as part of PC2 in Fig. 4(b), the phase indication is present when either PC1, PC2, or PC3 is used. The PCP<sub>out</sub> phase-lock condition is present because the inputs for SIG<sub>in</sub> and COMP<sub>in</sub> are in parallel. As noted in the waveforms of Fig. 4(b), PCP<sub>out</sub> at pin 1 of the HC/HCT4046A remains in a high state when the loop is phase locked. When either the PMOS or NMOS device is on, the PCP<sub>out</sub> is low. How the PCP<sub>out</sub> is used depends on the application. To fully utilize this output as a practical lock indicator, a smoothing filter is needed to reduce the effects of noise and marginal lock-in flicker.

##### Lock Detector of the HC/HCT7046A

Additional lock indicator circuitry has been added to the HC/HCT7046A, replacing the PC3 function with an improved lock detector and filter. As shown in the logic diagram for the HC/HCT7046A of Fig. 2(b), the PC2 circuit provides the same set of indicator signals as the PCP<sub>out</sub> circuit of the HC/HCT4046A, Fig. 2(a). Additional stages are used to process the lock-detection output signal (LD) of the HC/HCT7046A.

Detection of a locked condition is accomplished in the HC/HCT7046A with a NOR gate and an envelope detector, as shown in Fig. 6. When the loop is phase locked, the output of the NOR gate is high and the lock detector output (pin 1) is at a constant high level. As the loop tracks the SIG<sub>in</sub> on pin 14, the NOR gate generates pulses having widths that represent the phase difference between the COMP<sub>in</sub> (from the VCO) and SIG<sub>in</sub>. The time between pulses is approximately equal to the time constant (T) of the VCO center frequency. During the rise time of the pulse, the diode across the 1.5-kilohm resistor is forward biased, and the time constant in the path that charges the lock-detector capacitor (C<sub>LD</sub>) is given by:

$$T = (150 \text{ ohms} \times C_{\text{LD}})$$

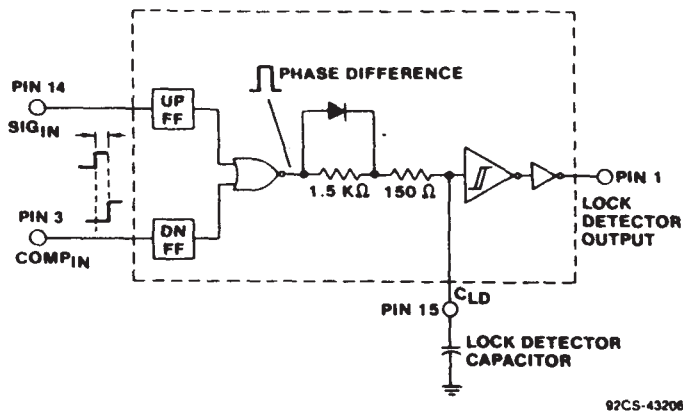


Fig. 6 - Lock-detector circuitry in the HC/HCT7046A.

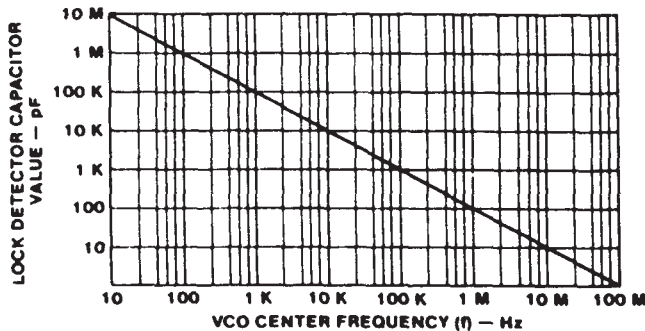


Fig. 8 - Selection chart for determining value of lock-detector capacitor.

The discharge circuit includes the 1.5-kilohm resistor. The capacitor waveform is a sawtooth, as shown in Fig. 7. The lock-detector capacitor value is determined by the center frequency of the VCO. The typical range of capacitance for a frequency of 10 megahertz is about 10 picofarads, and for a frequency of 100 kilohertz, about 1000 picofarads. The value of  $C_{LD}$  can be selected by means of the chart in Fig. 8. As long as the loop remains locked and tracking, the level of the sawtooth will not go below the switching threshold of the Schmitt-trigger inverter. If the loop breaks lock, the width of the error pulse will be wide enough to allow the sawtooth waveform to go below the threshold, and a level change at the output of the Schmitt-trigger will indicate a loss of lock, as shown in Fig. 9. The lock-detector capacitor also filters out small glitches that can occur when the loop is either seeking or losing lock.

As noted for the PCP<sub>out</sub> of the HC/HCT4046A, the lock-detector function of the HC/HCT7046A is present in any application of PC1, PC2, or PC3. However, it is important to note that, for applications using PC1, the lock detector will only indicate a locked condition on the fundamental frequency and not on the harmonics that PC1 may lock on. If a detection of lock is needed for the harmonic locking range of PC1, then the lock detector output must be OR-ed with the output of PC1.

#### VOLTAGE-CONTROLLED OSCILLATOR (VCO)

The High-Speed CMOS PLL ICs incorporate a versatile and easy-to-use VCO with a number of enhanced features

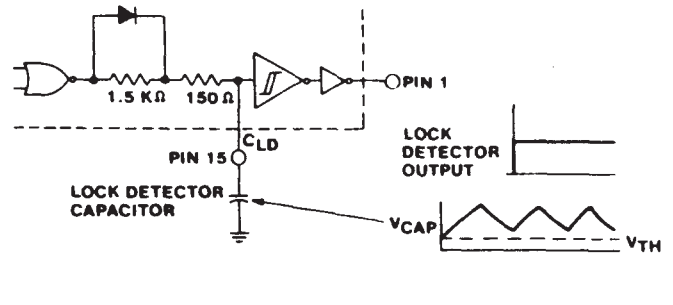


Fig. 7 - Waveform at lock-detector capacitor when in lock.

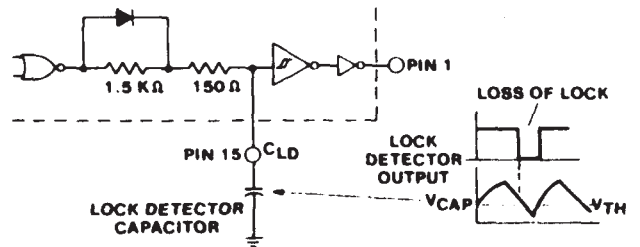


Fig. 9 - Waveforms at lock-detector capacitor when unlocked.

resulting from the High-Speed CMOS process. The most notable advantage is an order of magnitude increase in the VCO frequency range over that of the CD4046B.

The following VCO applications are intended to highlight problem solutions. Equations for the VCO frequency have been developed with emphasis on the high-frequency range. Graphical comparisons of measured and calculated frequency results are given.

#### VCO Description

Fig. 10 shows a functional diagram of the VCO control circuit of the HC/HCT4046A. The frequency and offset-frequency amplifiers are configured to convert voltage to current, which is then amplified in the current-mirror-amplifier (CMA) blocks before being summed. The summed current is directed to the oscillator section consisting of inverters  $G_1$  and  $G_2$ . The inverters, switching as H-drivers, control charge and discharge current to the oscillator range capacitor,  $C_1$ . The oscillator loop consists of flip-flop FF with feedback from the cross-coupled outputs to  $G_1$  and  $G_2$ . The demodulator output amplifier may be optionally used to buffer the filtered output of the phase comparator. In normal use, the load resistor  $R_L$  is in the range of 50 kilohms to 100 kilohms. An inhibit amplifier controls the oscillator and CMA circuits. The output from one side of the flip-flop is buffered and output to the VCO<sub>out</sub> at pin 4.

The external components  $R_1$ ,  $R_2$ , and  $C_1$ , plus the voltage level of VCO<sub>m</sub> at pin 9, provide direct control of the frequency. Resistors  $R_1$  and  $R_2$  fix the level of current bias to

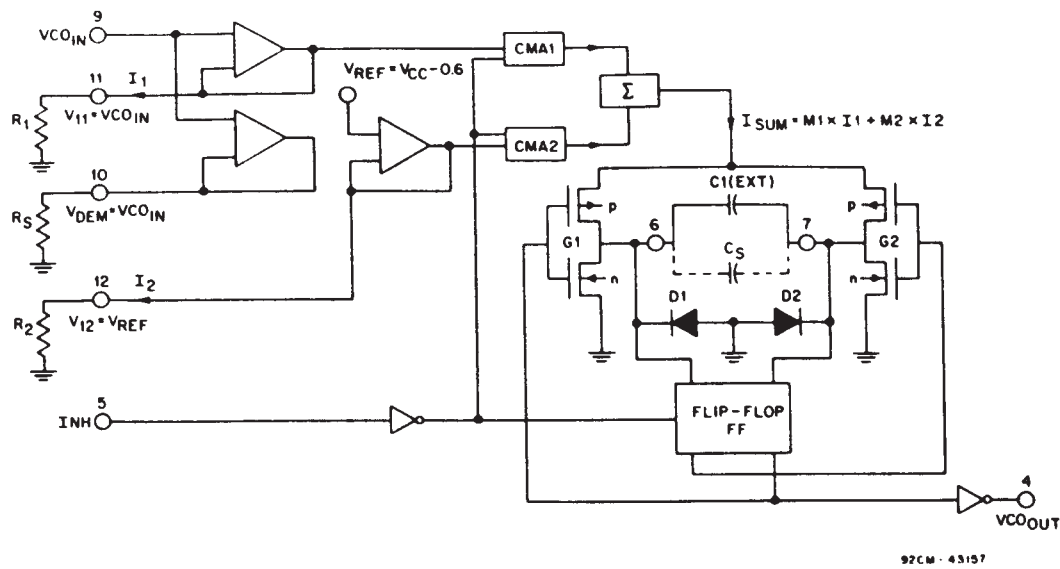


Fig. 10 - Functional block diagram of VCO portion of CD74HC4046A/7046A.

1A1 and CMA2 for currents  $I_1$  and  $I_2$ , respectively. Both  $\mu A$  circuits consist of a current mirror with, typically, 6 to 8 times gain. Because the frequency and offset-frequency amplifiers are source followers with 100% feedback, the voltage across  $R_1$  at pin 11,  $V_{R1}$ , is equal to  $V_{CO_{in}}$ , and the voltage across  $R_2$  at pin 12,  $V_{R2}$ , is equal to  $V_{REF}$ .  $V_{REF}$  is an internal bias source set at one forward diode drop from  $V_{CC}$ . As such, the voltage across  $R_2$  and the current  $I_2$  are functions of  $V_{CC}$ , implying the need for a well-regulated  $V_{CC}$  for good offset-frequency stability. For most applications,  $V_{REF} = V_{CC} - 0.6$  volt is a good approximation. In the equations that follow,  $I_1 = V_{CO_{in}}/R_1$  and  $I_2 = V_{REF}/R_2$  are used as direct expressions for the CMA input currents.

The outputs of CMA1 and CMA2 are the amplified  $M_1 I_1$  and  $M_2 I_2$  currents where  $M_1$  and  $M_2$  are the multiplier ratios for CMA1 and CMA2, respectively. The CMA output currents are then summed together as the current,  $I_{SUM}$ , to drive capacitor  $C_1$  via the PMOS and NMOS transistors of  $G_1$  and  $G_2$ . When the input to  $G_1$  is high, the input to  $G_2$  is low. In this mode, the PMOS transistor of  $G_1$  conducts charge to  $C_1$  while the NMOS transistor of  $G_2$  discharges the low side of  $C_1$  to ground. Each time the flip-flop changes state, the charging polarity of  $C_1$  is reversed by  $G_1$  and  $G_2$ . When the positively charged side of  $C_1$  is grounded, an intrinsic diode across each of the NMOS devices discharges  $C_1$  to one diode level below ground.

There are two  $C_1$  charge cycles in each full period, and the instantaneous start voltage for each current-charged ramp

is  $V_{tr} = -0.7$  volt. The active switch threshold at the flip-flop input is  $V_{tr} = 1.1$  volts for a  $V_{CC}$  of 5.0 volts, and varies with  $V_{CC}$  as shown in Figs. 11(a) and 11(b). Fig. 11(b) shows the voltage waveforms at pins 6 and 7 as similar except for the half-cycle displacement. The total peak-to-peak voltage of the sawtooth ramp waveform at pins 6 or 7 is typically  $V_{ramp} = [V_{tr} - V_{tr}] = [1.1 - (-0.7)] = 1.8$  volts.

#### VCO Frequency Control

When a capacitor,  $C$ , is charged with a constant current,  $I$ , the expression for the voltage,  $V_c$ , integrated over time,  $T_c$ , is:

$$V_c = (1/C) \int I dt = (IT_c)/C$$

In this case, the capacitor voltage is:

$$V_c = V_{ramp} = (V_{tr} - V_{tr}) = I_{SUM}(T_c/C_1) \quad (1)$$

or:

$$T_c = C_1 \times V_{ramp}/I_{SUM}$$

where  $I_{SUM} = [(M_1 I_1) + (M_2 I_2)]$ .

The time,  $T_c$ , is the ramp charge time, and  $V_{ramp}$  is the capacitor ramp charge voltage over the integrated time period. The ramp rate of voltage increase is  $V_{ramp}/T_c$ , and is determined by the rate of charge of the capacitor by the source current,  $I_{SUM}$ .



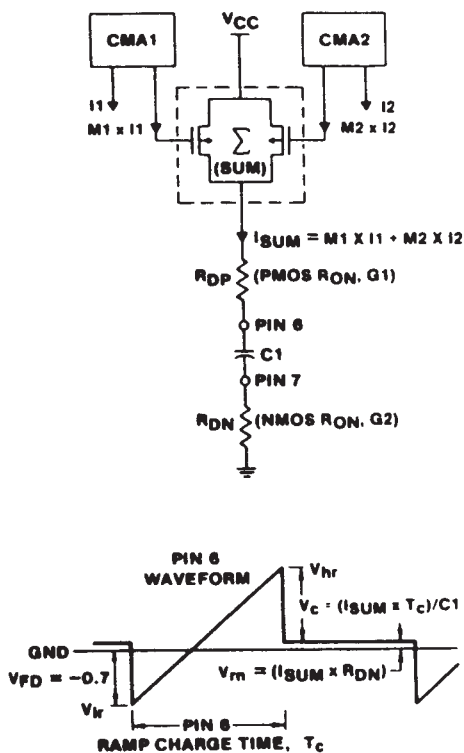


Fig. 11(a) - Equivalent HC/HCT4046A charge circuit of the voltage-controlled oscillator.

The CMA gain characteristics for  $M_1$  and  $M_2$  are shown in the curves of Figs. 12, 13, and 14. The values for  $M_2$  as a function of  $I_2$  are shown in Fig. 12. The curves of Fig. 13 show the CMA2 range of linearity for  $I_2$  input. The linear range and values for multiplier  $M_1$  are shown in the curves of Figs. 14(a) and 14(b).

Equation 1 is sufficiently accurate to allow a good approximation of the VCO period ( $2T_c$ ). However, there is a more precisely accurate equation for ramp charge time. In Fig. 11(b), Note 1, attention is called to an offset voltage of approximately 0.15 volt. Fig. 11(a) illustrates the reason for this characteristic in an equivalent circuit, where the mode of switching is for the  $G_1$  - PMOS and  $G_2$  - NMOS transistors in their "on" charge state. The more precise form of the voltage equation should include the NMOS channel resistance,  $R_n$ .

Because the trip point,  $V_{hr}$ , is the sum of  $V_c + V_m$ , and does not change in value, and  $V_{ir} = V_c(0)$  is approximately -0.7 volt as the initial charge condition on capacitor  $C_1$ :

$$V_{ramp} = V_{hr} - V_{ir} = (V_c + V_m) - V_c(0) = I_{sum} T_c / C_1$$

where:

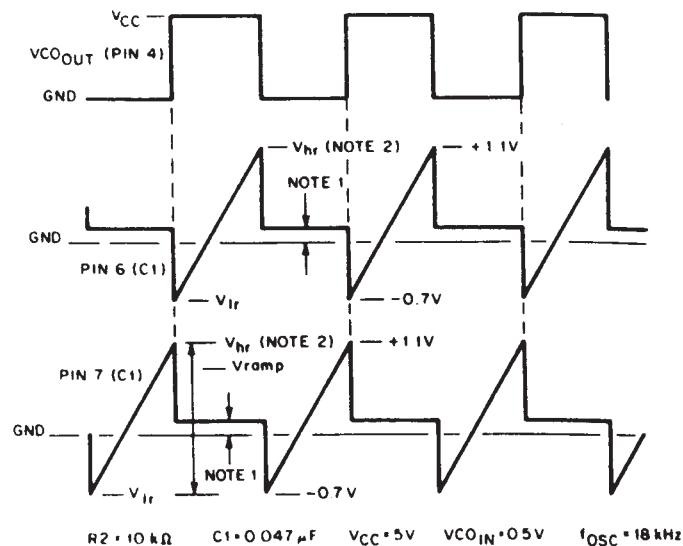
$$I_{sum} = (M_1 I_1) + (M_2 I_2)$$

and, because  $V_m = I_{sum} R_n$ :

$$T_c = (V_{ramp} - I_{sum} R_n) C_1 / I_{sum} \tag{2}$$

where  $V_{ramp}$  is the same as defined in Equation 1.

As noted above, the initial voltage,  $V_c(0)$  is one diode drop below ground, or -0.7 volt, and is equal to  $V_{ir}$ . The  $V_{hr}$  trip



- NOTES  
 1 THE 0.15 VOLT OFFSET AT PIN 6, 7 IS DUE TO CHARGE CURRENT TIMES DRAIN-TO-SOURCE SATURATED ON-RESISTANCE IN THE N-CHANNELS OF  $G_1$ ,  $G_2$  NMOS TRANSISTORS  
 2  $V_{hr}$  VARIES WITH  $V_{CC}$  WHERE  $V_{hr} = (0.1V_{CC} + 0.6)$  VOLTS

92CS-43159

Fig. 11(b) - HC/HCT4046A voltage-controlled-oscillator waveforms.

point for the flip-flop does not change, and was noted to be typically 1.1 volt for  $V_{CC} = 5$  volts. As shown in Fig. 11(a),  $V_{hr} = V_c + V_m$ . This expression shows that less charging time is needed to reach the trip point because  $V_c$  is reduced by the  $I_{sum} R_n$  voltage drop. The  $I_{sum} R_n$  term introduces a characteristic of nonlinear increasing frequency as a function of

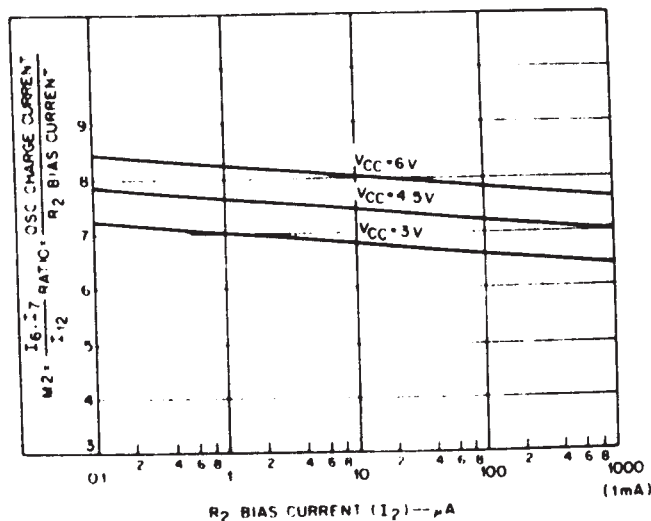


Fig. 12 - Current multiplier ratio  $M_2$  as a function of  $R_2$  bias current.

92CS-43160

92CS 43210

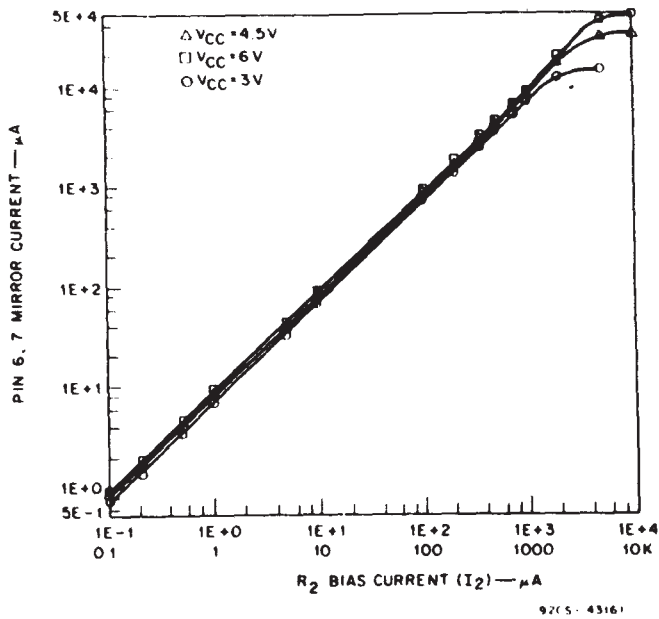


Fig. 13 - Mirror current as a function of  $R_2$  bias current showing range of linearity.

$V_{COin}$  voltage and is caused by the voltage drop in the NMOS channel resistance. When  $V_{COin}$  is increased, the added  $M_{11}$  current continues to further reduce the sweep-  
 requirement. For large values of  $R_1$  and  $R_2$ , the effect of  
 resistance  $R_n$  is small, and the  $V_{in}$  term in the above  
 equations may be neglected.

When Equation 1 or 2 is used as a first-order approximation, a complete expression for frequency would incorporate

timing for two ramps, plus the propagation delays for each flip-flop state, plus the added time for charging stray capacitance. Either case yields a ramp charge expression. The propagation delay,  $T_{pd}$ , is a function of the number of cascaded stages in the flip-flop, plus  $G_1$  and  $G_2$  switching propagation-delay times. The stray capacitance,  $C_s$ , from pin 6 to 7 (or from each pin to ground) must be added to the value of  $C_1$ . It should be noted that unbalanced capacitance to ground from pin 6 and pin 7 can contribute an unbalanced duty cycle. In fact, unbalanced capacitance at pins 6 and 7 may be used by design to correct or set the duty cycle. With the frequency-dependent parameters now defined, the VCO frequency becomes:

$$f_{osc} = 1/T_{osc} = 1/(2T_c + 2T_{pd}) \quad (3)$$

Using the simplified expression of Equation 1 to calculate the ramp charging time, and including the appropriate terms for capacitance  $C_1 + C_s$ ,  $V_{ramp}$ , and  $I_{sum}$ :

$$T_c = [(C_1 + C_s) \times V_{ramp}] / [(M_1 I_1) + (M_2 I_2)]$$

which expands to:

$$T_c = [(C_1 + C_s) V_{ramp}] / [M_1 (V_{COin}/R_1) + M_2 (V_{ref}/R_2)] \quad (4)$$

where:

$$I_{sum} = [M_1 (V_{COin}/R_1) + M_2 (V_{ref}/R_2)]$$

The more precise solution is:

$$T_c = [(C_1 + C_s) (V_{ramp} - I_{sum} R_n)] / I_{sum} \quad (5)$$

The value of  $T_c$  is calculated from Equation 4 or 5, and is substituted into Equation 3 to determine the frequency,  $f_{osc}$ . For the most part, Equations 3 and 4 provide a reasonably accurate and direct approach to determination of the frequency of the VCO in terms of external component values and known parametric voltage values.

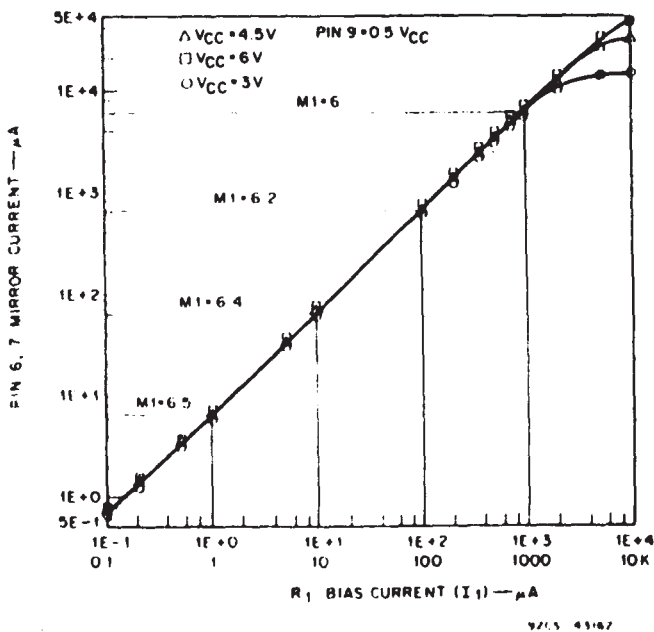


Fig. 14(a) - Mirror current as a function of  $R_1$  bias current showing range of linearity.  $V_{COin}$  (pin 9) voltage is  $0.5 V_{CC}$ .

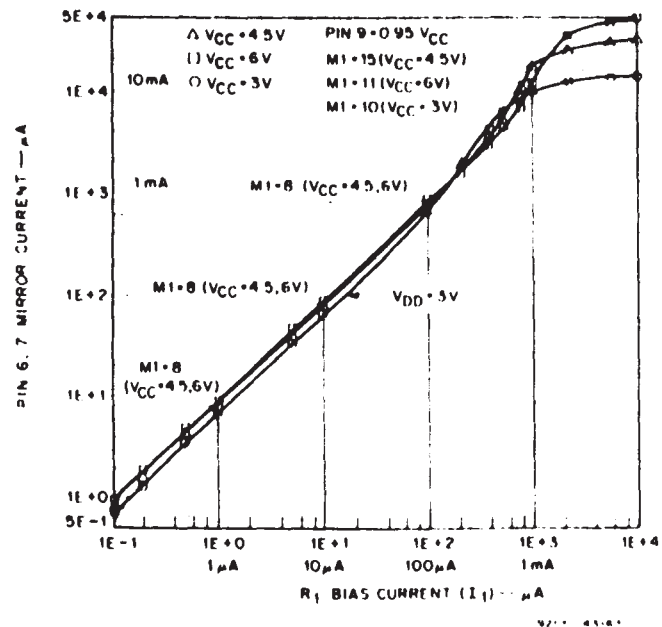


Fig. 14(b) - Mirror current as a function of  $R_1$  bias current showing range of linearity.  $V_{COin}$  (pin 9) voltage is  $0.95 V_{CC}$ .

### VCO Parametric Ranges and Restrictions

When Equations 3 and 4 or 5 are used, it is necessary to adhere to certain range limitations for the components and to seek the correct parametric values for other variables. The following list tabulates the variables of the equations and defines ranges and restrictions.

$V_{CC}$	Defined in the HC/HCT4046A and HC/HCT7046A data sheets as 7 volts maximum - for normal operation should remain in the range of 3 to 6 volts.
$V_{COin}$	The pin 9 voltage, $V_{COin}$ , determines the frequency of the VCO. The control range is 1.0 volt $< V_{COin} < 0.9V_{CC}$ ; the VCO will become unstable if $V_{COin}$ exceeds the maximum. On the low side, the VCO is not responsive to input level until $V_{COin}$ is $\geq 1.0$ volt.
$V_{ref}$	The internal reference voltage, $V_{ref}$ , is equal to one forward diode drop below $V_{CC}$ ( $V_{CC} - 0.6$ volt). Where $R_2$ is used to fix offset frequency by current $I_2$ , the $V_{ref}$ level is maintained at pin 12 ( $R_2$ ) to set the source current, $I_2$ .
$V_{ramp}$	Values for $V_{ramp}$ are defined above with commentary on the effect of $I_{sum}R_n$ which, for many applications, is a second-order effect and can be neglected. As an empirically derived equation, $V_{hr} = (0.1V_{CC} + 0.6)$ volts and $V_{ramp} =  (V_{hr} - V_{tr})  = (0.1V_{CC} + 1.3)$ volts.
$C_1$	The external VCO timing capacitor between pins 6 and 7 should be greater in value than 40 picofarads. Lower values will be subject to device and layout tolerance variations caused by the stray capacitance at pins 6 and 7.
$C_s$	Stray capacitance at pins 6 and 7 is not limited to pin-to-pin capacitance. Any stray capacitance at pin 6 or pin 7 must be charged and discharged during each normal oscillator cycle.
$R_1$	The value of $R_1$ determines the frequency of the VCO for the defined $V_{COin}$ range. Note that the

minimum (offset) frequency is determined by  $R_2$ , and that the current in  $R_1$  is determined by  $I_1 = V_{COin}/R_1$ .

$R_2$	$R_2$ is frequently misused. The value of $R_2$ determines the offset (minimum) frequency of the oscillator. When there is no basic need for an offset frequency, $R_2$ should be omitted. If it is, no termination is needed at pin 12. When $R_2$ is not used, and if the detector reference signal is removed, the oscillator's minimum frequency drops to zero. To sustain oscillation during signal dropout, some value of $R_2$ is needed. The current in $R_2$ is determined by $I_2 = V_{ref}/R_2 = (V_{CC} - 0.6)/R_2$ .
$M_1, M_2$	The currents $I_1$ in resistor $R_1$ and $I_2$ in resistor $R_2$ are multiplied in the current mirrors CMA1 and CMA2 and summed to provide the $I_{sum}$ charging current to $C_1 + C_s$ . The CMA multiplying factors are, respectively, $M_1$ and $M_2$ . Fig. 12 provides curve families for $M_2$ as a function of $I_2$ and $V_{CC}$ . The nominal current-multiplier factor for $M_1$ is determined from the curves of Fig. 14(a).
$I_{sum}$	Where $I_{sum}$ is defined as $(M_1I_1 + M_2I_2)$ , the total sum of $I_1 + I_2$ should not exceed 1.0 milliampere. The multiplier values of $M_1$ and $M_2$ are typically 6 to 8 times. At higher levels of current, $I_{sum}$ will degrade VCO linearity. The limits of linear range in the curves of Figs. 13 and 14 should be noted.
$T_{pd}$	Inherent propagation delay as noted in Equation 3 is approximately 10 to 14 nanoseconds for the flip-flop in the feedback loop of the oscillator. For $V_{CC}$ levels of 7 volts, the propagation delay decreases approximately 10%. For 3 volts, the propagation delay increases approximately 30%.
$T_c$	The ramp charge time, $T_c$ , for capacitor $C_1$ is assumed to be equal for pin 6 to 7 or pin 7 to 6 in Equations 4 and 5.
$f_{osc}$	The oscillator frequency for a given $V_{COin}$ as read at the $V_{COout}$ , pin 4. It may be calculated by means of Equations 3 and 4 or 5.

### DESIGN EXAMPLES WITH MEASURED AND CALCULATED RESULTS

The curves of Fig. 15(a) illustrate test-measurement data for the HC/HCT4046A for frequency,  $f_{osc}$ , as a function of  $V_{COin}$  voltage. Using  $R_1 = R_2 = 10$  kilohms,  $C_1 = 47$  picofarads,  $C_s = 6$  picofarads, and assuming  $T_{pd} = 11$  nanoseconds in the circuit of Fig. 15(b), curves for  $V_{CC}$  values of 3, 4, 5, and 6 volts were measured and plotted. The dashed lines for the curves B, D, and E were calculated using Equations 3 and 4 and illustrate that there is a

reasonable agreement of measured and calculated results. The effect of an accelerated frequency increase is more noticeable in the  $V_{CC} = 5$  volts curve (curve E) with no offset (no  $R_2$ ), where the measured frequency sweeps up with an increasing slope. The approximation equations, however, are still valid, varying from 5 to 15% error, mostly at the high  $V_{COin}$  voltage values. The effects of no offset bias should be noted in the curve for  $V_{CC} = 5$  volts and  $R_2 = \text{infinity}$  (curve E). Without offset bias, all oscillation stops when the  $V_{COin}$  voltage drops below 1.0 volt

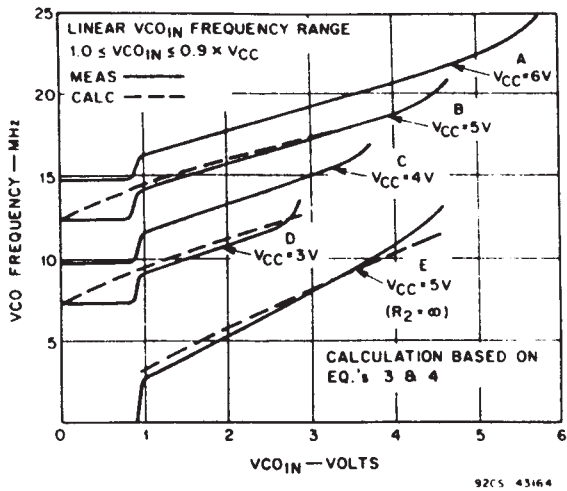


Fig. 15(a) - VCO frequency as a function of input voltage VCO<sub>in</sub>. Both measured and calculated values are shown.  $R_1 = R_2 = 10k\Omega$ ,  $C_1 = 47pF$ ,  $C_s = 6pF$ ,  $T_{pd} = 11ns$  @  $V_{cc} = 5V$ , and  $T_{pd} = 15ns$  @  $V_{cc} = 3V$ .

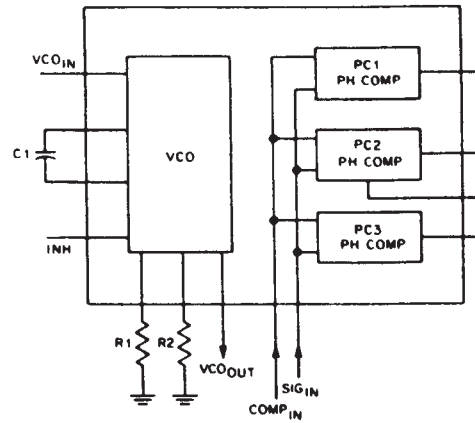


Fig. 15(b) - Test circuit for HC/HCT4046A phase-locked loop VCO.

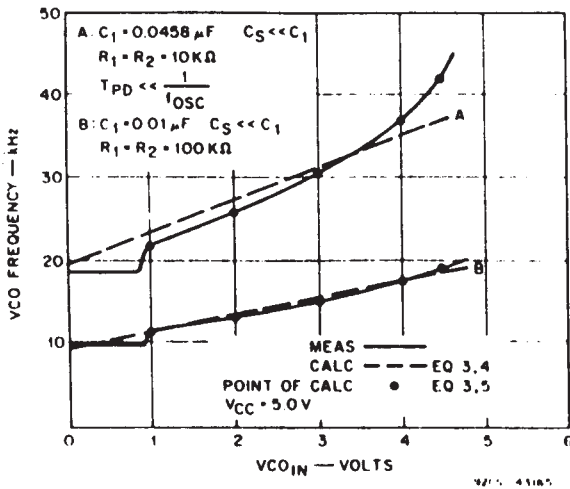


Fig. 16 - VCO frequency as a function of input voltage VCO<sub>in</sub> showing effects of different values of  $R_1$  and  $R_2$  (10 and 100 kilohms).

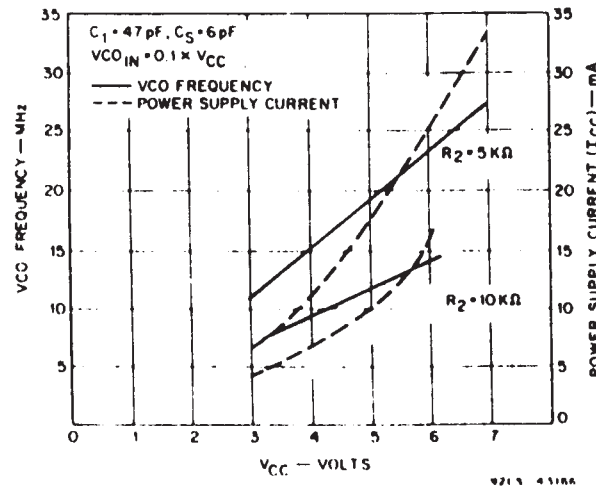


Fig. 17 - VCO frequency and power supply current as a function of operating voltage V<sub>cc</sub> showing effects of different values of  $R_2$  (5 and 10 kilohms).

Although values of 10 kilohms for  $R_1$  and  $R_2$  provide good linearity as a function of VCO<sub>in</sub> for the high-frequency range shown in Fig. 15(a), optimum values for  $R_1$  and  $R_2$  are greater at lower frequencies. This fact is illustrated in the curves of Fig. 16, where the linearity is shown to be better for the larger values of  $R_1$  and  $R_2$  (curve B). The accelerated frequency-increase effect of  $I_{sum}R_n$  is more pronounced. The propagation delay is neglected in the curves of Fig. 16 because it is much less than the oscillator period. The effects of stray capacitance are neglected for similar reasons. The simplified solutions using Equations 3 and 4 are shown by the dash lines.

A more accurate calculation was made with Equations 3 and 5 to determine the value of  $I_{sum}$ . A value of 50 ohms was

used to calculate the  $I_{sum}R_n$  term. The calculated results for this curve quite accurately overlay the measured, solid-line curves. In this calculation, the values of  $M_1$  and  $M_2$  were set 15% low to obtain the exact tracking match.

The curves of Fig. 17 show measured data and illustrate the dependence of the offset frequency on V<sub>cc</sub>. The frequency is in megahertz and the power supply current in milliamperes. These parameters are plotted against power-supply voltage. I<sub>cc</sub> is shown for  $R_2$  offset frequency bias resistors of 5 and 10 kilohms. The supply current increases with a decrease in the value of resistor  $R_2$ , and also increases with the switching frequency because of the added current needed to charge and discharge the device equivalent capacitance,  $C_{pd}$ .

The curves of Fig. 18 show the effect of increasing the values of resistors  $R_1$  and  $R_2$  by ten times with all other factors remaining the same. Curve A is plotted at 10 times the measured frequency, while curve B is plotted at the frequency of the measured data. The two curves should overlay one another. The current multiplier ratios, however, are higher at lower current bias levels, a factor that causes the frequency defined by curve A to be slightly more than ten times that of curve B. The curves illustrate that frequency can be changed by a linear scale factor with a change in  $R_1$  or  $R_2$ . Similar frequency changes may also be made by adjustment of  $C_1$ . An exception to be noted is that effects of  $T_{pd}$  and  $C_s$  will produce a ratio adjustment error in the high-frequency range. Fig. 19(a) demonstrates the results of a different method of frequency control by "splitting" capacitor  $C_1$  and returning pin 6 and pin 7 separately through capacitors  $C_{1A}$  and  $C_{1B}$  to ground. Illustrated in Fig. 19(b), this method has the facility to control the duty cycle, which is the ratio of capacitors  $C_{1A}$  and  $C_{1B}$ . The  $V_{ramp}$  conditions change from -0.7 volts as a starting point to ground or zero volts. The  $V_{hr}$  trip point is unchanged. The current charge path for each capacitor is through its respective  $G_1$  or  $G_2$  PMOS device, and the discharge path is through the associated NMOS device. Frequency calculations for this type of circuit are based on a separate calculation for each capacitor charge ramp and the addition of the results for the total period time. The same equations are used in the calculations, but the empirical equation for  $V_{ramp}$  becomes:

$$V_{ramp} = V_{hr} - V_{lr} = 1.1 - 0 = 1.1V$$

where  $V_{CC} = 5.0$  volts.

For other  $V_{CC}$  values,  $V_{hr} = (0.1V_{CC} + 0.6)$  volts. The simplified calculation is shown by the dashed line in Fig. 19(a) to be in reasonable agreement with empirical results. Where the RC discharge may not reach ground before the charge cycle starts,  $V_{lr} = V_c(0)$  assumes this value. The waveform characteristic is shown in Fig. 19(b).

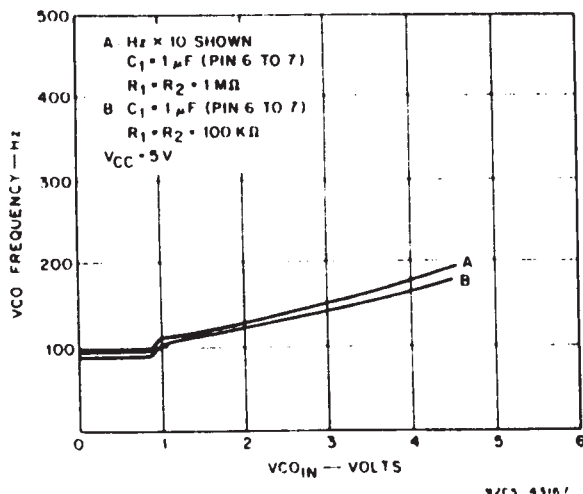


Fig. 18 - VCO frequency as a function of input voltage  $V_{CO,IN}$  showing effects of different values of  $R_1$  and  $R_2$  (10 kilohms and 1 megohm).

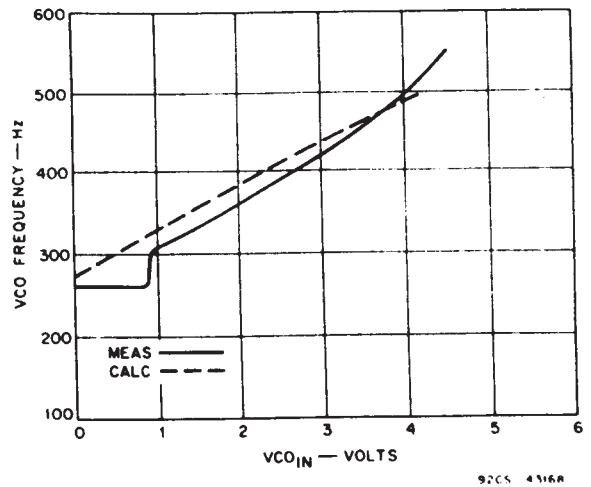


Fig. 19(a) - VCO frequency as a function of input voltage  $V_{CO,IN}$  showing duty cycle control obtained by splitting capacitor  $C_1$  and controlling ratio of  $C_{1A}$  and  $C_{1B}$ .

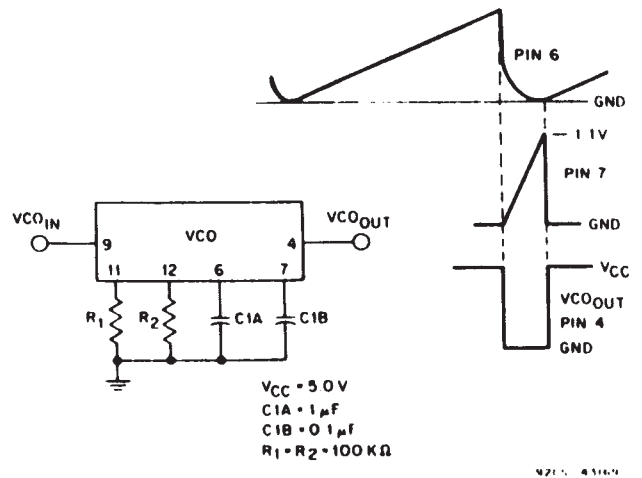


Fig. 19(b) - Evaluation circuit and waveforms for the Fig. 19(a) curve.

Possible applications of the split-capacitor method described above include horizontal and vertical timing circuits for image display systems as well as gating and blanking functions where, for a variety of reasons, pulse-width control may be needed.

**DESIGN EXAMPLES WITH AND WITHOUT OFFSET**

The equations derived thus far have provided a means to calculate frequency. However, frequency is usually the known parameter. If it is not known, an approximation may be initially calculated, followed by an iterative adjustment for the final desired result. Dynamic range limitations may be more easily accommodated by following this procedure



### Example No. 1 With Offset

For a supply voltage  $V_{CC} = 5$  volts and given:

$$\begin{aligned} f_o \text{ (center frequency)} &= 400 \text{ kHz} \\ f_{\min} \text{ (offset frequency)} &= 250 \text{ kHz} \\ f_{\max} &= f_o + 2(f_o - f_{\min}) = 550 \text{ kHz} \end{aligned}$$

The curves plotted thus far indicate that a value of 0.01 microfarad may be a suitable value for  $C_1$ , and that propagation delay and stray capacitance may be neglected. For convenience, assume that the multiplying factor  $M = M_1 = M_2 = 7.2$  and, from previously noted values,  $V_{\text{ramp}} = 1.8$  volts. First calculate the offset frequency by setting  $V_{CO_{in}} = 0$  volts. With these simplified conditions, Equations 3 and 4 become:

$$f_{\min} = 1/2T_c = 1/2(C_1 V_{\text{ramp}}/M_2 I_2)$$

or:

$$f_{\min} = 2M_2 V_{\text{ref}}/C_1 V_{\text{ramp}} R_2$$

where  $I_2 = V_{\text{ref}}/R_2 = (V_{CC} - 0.6)/R_2 = 4.4/R_2$ .

Solving for  $R_2$  yields:

$$\begin{aligned} R_2 &= M_2 V_{\text{ref}}/2C_1 V_{\text{ramp}} f_{\min} \\ &= (7.2 \times 4.4)/(2 \times 0.01 \mu\text{F} \times 1.8 \times 250 \text{ kHz}) \\ &= 3.52 \text{ kilohms} \end{aligned}$$

If this low value of  $R_2$  is used, the resultant  $I_{\text{sum}} R_n$  will cause pronounced nonlinearity, as shown in Fig. 16, curve A. Better linearity can be achieved with an  $R_2$  of 35.2 kilohms by scaling frequency;  $C_1$  can also be set to 1000 picofarads. This choice seems practical because the assumption is that stray capacitance,  $C_s$ , is 6 picofarads, which is not a significant percentage of  $C_1$ .  $R_2$  should be further adjusted by choosing a value for it of 36 kilohms, which is close to a standard value of resistance.

From the known maximum frequency,  $f_{\max}$ , and given the value of  $R_2$ ,  $R_1$  may be calculated. Assume that the maximum frequency will occur at approximately  $V_{CO_{in}} = V_{\text{ref}} = 4.4$  volts. The same values of  $M_1$  and  $M_2$  as used above will continue to be used for this approximation. The problem now is to find a parallel value of  $R_1$  and  $R_2$  ( $R_{\text{eq}}$ ) for the calculation of  $f_{\max}$  where:

$$\begin{aligned} R_{\text{eq}} &= M V_{CO_{in}}/2C_1 V_{\text{ramp}} f_{\max} \\ &= (7.2 \times 4.4)/(2 \times 1000 \text{ pF} \times 1.8 \times 550 \text{ kHz}) \\ &= 16 \text{ kilohms} \end{aligned}$$

For  $R_2 = 35.2$  kilohms,  $R_1$  is determined to be 29.3 kilohms, or approximately 30 kilohms to the nearest standard value. With these values and Equations 3 and 4, the calculations for the frequency can be fine tuned. With  $V_{\text{ref}}/R_2$  at 122 microamperes,  $M_2$  from Fig. 12 becomes 7.3. Similarly, when  $V_{CO_{in}} = V_{CC}/2$ ,  $V_{CO_{in}}/R_1 = 83$  microamperes, which, from Fig. 14(a), yields  $M_1 = 6.2$ .

$T_c$  and  $f_{\text{osc}}$  as a function of  $V_{CO_{in}}$  can be calculated from these values and, if needed,  $R_1$  and  $R_2$  can be adjusted to meet the desired center-frequency condition. That is, for  $C_s = 0$ ,  $T_{\text{pd}} = 0$ ,  $R_1 = 30$  kilohms,  $R_2 = 36$  kilohms,  $C_1 = 1000$  farads,  $V_{\text{ref}} = 4.4$  volts,  $V_{\text{ramp}} = 1.8$  volts,  $M_1 = 6.2$ ,  $M_2 = 7.3$ , and  $V_{CC} = 5$  volts:

$$\begin{aligned} f_{\text{osc}} &= 1/2T_c = [M_1(V_{CO_{in}}/R_1) + M_2(4.4/R_2)]/2C_1 V_{\text{ramp}} \\ &= [6.2(V_{CO_{in}}/30 \text{ kilohm}) \\ &\quad + 7.3(4.4/36 \text{ kilohm})]/(2 \times 1000 \text{ pF} \times 1.8 \text{ V}) \end{aligned}$$

The table below gives calculated and measured oscillator frequency values for different values of  $V_{CO_{in}}$ .

VCO <sub>in</sub> (V)	f <sub>osc</sub> (kHz)	
	Calculated	Measured
0.0	248	280
1.0	305	318
2.5	391	384
4.4	500	492

The calculated solution is in reasonable agreement with the desired results as shown by the measured data. Depending on the application, some adjustment of  $R_2$  may more closely fit the  $f_{\text{osc}}$  value.

### Example No. 2 - Without Offset

Given:  $f_o = 400$  kilohertz,  $V_{CC} = 5.0$  volts

Without offset, the calculation is simplified to:

$$f_{\text{osc}} = 1/2T_c = M_1(V_{CO_{in}}/R_1) / 2C_1 V_{\text{ramp}}$$

Drawing on the experience of the previous calculation,  $M_1$  is approximately 6.2 and  $V_{CO_{in}}$  is set to 2.5 volts for the center-frequency calculation. Solving for  $R_1$ :

$$\begin{aligned} R_1 &= 6.2(2.5/f_o) / 2 \times 1000 \text{ pF} \times 1.8 \text{ V} \\ &= 10.8 \text{ kilohms} \end{aligned}$$

Using 11 kilohms for  $R_1$ , gives:

VCO <sub>in</sub> (V)	f <sub>osc</sub> (kHz)	
	Calculated	Measured
1.0	157	139
2.5	391	352
4.4	699	697

In this example the error is larger, but the dynamic range needed for the high and low end of the frequency range is there. The center-frequency value of  $V_{CO_{in}}$  is slightly to the high side of 2.5 volts.

### "THUMB RULES" FOR QUICK CALCULATIONS

The above two examples imply that simple equations and "thumb-rules" can be effectively applied to the determination of required parameters. Designers, however, should remain alert to the fact that large values of  $I_{\text{sum}}$  with frequencies in the megahertz range do require use of the expanded Equations 3, 4, and 5. For extreme ranges of current and voltage, other errors may be added. However, reasonable approximations of the offset frequency,  $f_{\min}$ , and the maximum frequency,  $f_{\max}$ , can be made. Where  $T_{\text{pd}} \ll 1/f_o$  or the frequency range is less than 1.0 megahertz and the  $I_{\text{sum}}$  currents are reduced so that  $I_{\text{sum}} R_n \ll V_{\text{ramp}}$ , the errors will generally be less than 15%. The quick-approximation equations are derived as follows:

From Equation 4, solving for  $f_{\min} = 1/2T_c$  at  $V_{CC} = 5$  V,  $V_{CO_{in}} = 0$  V,  $C_s = 0$  pF,  $V_{\text{ramp}} = 1.8$  V, and  $M_1 = M_2 = 7$  yields:

$$f_{\min} = K_o/(R_2 C_1) \quad (8(a))$$

where  $K_o$  is a constant that varies with  $V_{CC}$ .

To find  $f_{\max}$  with  $V_{CO_{in}} = V_{\text{ref}} = 4.4$  V,  $V_{CC} = 5$  V,  $C_s = 0$  pF,  $V_{\text{ramp}} = 1.8$  V, and  $M_1 = M_2 = 7$ :

$$f_{\max} = K_o/(R_{\text{eq}} C_1) \quad (8(b))$$

where  $R_1$  in parallel with  $R_2$  is equal to  $R_{eq}$ . Then, an extrapolation from  $f_{min}$  at  $VCO_{in} = 0$  to  $f_{max}$  at  $VCO_{in} = 4.4$  volts yields a quick  $y = mx + b$  equation approximation to  $f_{osc}$ :

$$f_{osc} = [(f_{max} - f_{min})/K_b]VCO_{in} + f_{min} \quad (6(c))$$

where  $K_b$  at  $f_{max}$  is 4.4 for  $V_{CC} = 5$  V or 5.4 for  $V_{CC} = 6$  V.  $K_a$  at  $f_{max}$  and  $f_{min}$  is 8.5 for  $V_{CC} = 5$  V and 10 for  $V_{CC} = 6$  V.

The solution is provided as a time constant for  $R_2C_1$  or  $R_{eq}C_1$ , where  $C_1$  is assumed, followed by a calculation for  $R_1$  and  $R_2$ .

The choice of offset frequency is not as simple as it first appears. The true offset with respect to phase lock starts when the  $VCO_{in}$  is approximately 1.0 volt. The lock-in range where  $2f_i = (f_{max} - f_{min})$  is limited by this condition. As such, the lock-in range is only 60% of the  $VCO_{in}$  control range for  $VCO_{in} = 0$  V to  $VCO_{in} = 2.5$  V or ( $V_{CC}/2$ ). Using the lower VCO control range as a boundary condition for lock-in,  $0.6(f_o - f_{min}) = f_i$ .

Where  $f_{min}$  is the offset frequency, the thumb-rule equation for offset in terms of center frequency and lock range is:

$$f_{min} = f_o - 1.6f_i \quad (6(d))$$

## TABULATED SOLUTIONS

The expanded Equations 1 through 5 have been written into a computer program using empirically derived equations from the curves and data for  $I_1$ ,  $I_2$ ,  $M_1$ ,  $M_2$ , and  $T_{pd}$ . This program is included in Appendix III. PC calculations and thumb-rule solutions have been calculated and compared to measured data to evaluate the frequency error in several applications. Appendix IV gives  $R_1$ ,  $R_2$ , and  $C_1$  values with "Calc.  $f_{osc}$ " PC solutions from Equations 3, 4, and 5. The "Approx.  $f_{osc}$ " values are given by the thumb-rule solutions from Equations 6(a), 6(b), and 6(c). The solutions shown below are based on high and low inputs to  $VCO_{in}$ , and have larger estimate errors than those previously shown and plotted. The most accurate frequency calculations are determined by having the correct values for  $M_1$  and  $M_2$ , which, for the full range of  $VCO_{in}$ , are not constant. The preferred solutions are derived for a  $VCO_{in}$  voltage near  $V_{CC}/2$ , where the curves for  $I_1$  as a function of pin 6 and pin 7 current plots are most accurate. The example data given here is based on single result values from constructed PC boards (see Appendix V).

## FILTER DESIGN FOR THE HC/HCT4046A

The third element of the HC/HCT4046A PLL to be discussed is the filter requirements for proper operation of the loop. An understanding of various technical terms is assumed. For further assistance, the reader is referred to Appendix I and the bibliography. It is important to remember that the filter characteristic is a key factor in determining the overall gain and phase response of the loop. Stability criteria is covered in general references on feedback theory along with other subjects including Bode plots, root-locus plots, and Nyquist criteria. The use of Laplace transforms with partial fraction expansions, the final value theorem, and other techniques should be very helpful to the dedicated designer of PLL circuits. Loop equations in Fig. 20 are expressed in terms of the complex frequency domain

Three basic types of low-pass filter (LPF) are commonly used in PLL circuits. All LPFs perform the basic function of

removing high-frequency components resulting from the multiplier process of the phase comparator. Fig. 20 shows these common forms of the LPF along with equations for the loop as applied to PLLs of second-order systems.

Another characteristic of the PLL is phase jitter, which may occur because the VCO is frequency modulated by the ripple output of the LPF. Moreover, noise may initiate fast changes in phase error and cause conditions of variable damped oscillation in the loop. Characteristics common to the PLL are noted in the following discussion, which also provides examples and data.

The LPF integration properly determines the time constant of the filter and affects the loop during frequency acquisition. A low-leakage termination for the filter provides a constant dc level to the VCO and maintains a minimum phase-shift relation between the VCO signal and the PLL input signal. The HC/HCT4046A features a very high resistance load to the LPF where the input resistance of the VCO is of the order of  $10^{12}$  ohms. In many applications, particularly at high frequency, leakage currents can cause an unacceptable phase error.

Loops are frequently referred to by type and order designation. Type is less commonly used and refers to the number of perfect integrators in the loop or the number of poles at the origin of the complex frequency plot. An example of a Type I would be a simple first-order PLL where there is no filter [ $f(s) = 1$ ]; integration of the VCO provides the one pole. The order of the loop is a more commonly used term and refers to the highest power of  $s$  in the denominator of the closed loop transfer function,  $H(s)$ . The application examples that follow are based on second-order systems, which represent the most common use of PLL circuits employing the HC/HCT4046A.

## LOOP EXAMPLES

### 1. Low-Pass Filter Using PC1

This first example illustrates the effects of parameter variation; PC1 and the simple RC lag LPF of Fig. 20(a) are used. The given conditions for this example are:

$$f_o = 27.5 \text{ kHz and } f_{min} = ? \text{ kHz} \\ V_{CC} = 6 \text{ V, } VCO_{in} \text{ range is 1 to 5.5 V}$$

The tendency for the novice designer is to specify an offset frequency close to the desired center frequency. This choice reduces the VCO gain factor and adds a resistor to the circuit. The need for an offset frequency specification should always be questioned. Occasionally, an offset frequency may be needed if the application requires continuing oscillation when the  $VCO_{in}$  input drops below 1.0 volt. The arbitrary assumption in this example is the choice of  $f_{min} = 0$  or no offset.

To find the VCO parameters, the designer should initially calculate  $R_1$  and  $C_1$  by considering the  $VCO_{in}$  level at  $V_{CC}/2$  or 3 volts. For this working frequency range, the consideration of stray capacitance and propagation delay can be dropped. Using the thumb-rule equation developed in the VCO section, the  $y = mx + b$  equation form can be used for  $f_{min} = 0$  and  $V_{CC} = 6$  V, where  $K_a = 10$  and  $K_b = 5.4$ . Then,  $R_{eq}$  reduces to  $R_1$ , and Equations 6(b) and 6(c) combine as:

$$f_{osc} = VCO_{in}/(0.54R_1C_1)$$

By choosing  $C_1 = 0.012$  microfarad,  $R_1$  becomes 16.8

actual component values used were  $R_1 = 16.4$  kilohms and  $C_1 = 0.012$  microfarad. Frequency calculations for a  $VCO_{in}$  of 1 and 3 volts using the above equation are as follows:

VCO <sub>in</sub> (V)	f <sub>osc</sub> (kHz)	
	Calculated	Measured
1.0	9.4	—
1.24	11.7	10
3.0	28.2	—
3.34	31.4	27.5

The values shown are a reasonable approximation of the required values.

The VCO gain factor,  $K_o$ , must be determined for the filter design. Either the slope of the curve for  $f_{osc}$  as a function of  $VCO_{in}$  can be used or a value can be calculated from the differentiated frequency expression. If  $I_{sum}R_n \ll V_{ramp}$ , then the  $I_{sum}R_n$  term may be dropped. In this case, the calculated error is approximately 3% at  $VCO_{in} = V_{CC} / 2$ . Using Equations 3 and 4, substituting  $T_c$  into the  $f_{osc}$  equation, and dropping the  $I_{sum}R_n$  and  $T_{pd}$  terms yields:

$$f_{osc} = I_{sum} / 2C_1V_{ramp} = M_1VCO_{in} / 2R_1C_1V_{ramp}$$

The differential with respect to  $VCO_{in}$  is given by:

$$K_o = d(f_{osc}) / d(VCO_{in}) = M_1 / 2R_1C_1V_{ramp}$$

result is the same as the differential of  $VCO_{in} / (0.54R_1C_1)$  if  $M_1 = 7$  and  $V_{ramp} = 1.9$  volts are assumed.

Substituting values  $M_1 = 7$ ,  $V_{ramp} = 1.9$  volts,  $R_1 = 16.4$  kilohms, and  $C = 0.012$  picofarad yields:

$$K_o = 9.4 \text{ kilohertz/volt or } 59.1 \text{ kiloradians/volt}$$

The  $K_d$  gain factor for the PC1 detector can then be calculated as:

$$K_d = V_{CC} / \pi = 6 / 3.1416 = 1.91 \text{ volts/radian}$$

The loop gain factor, not including the filter, is given by:

$$K = K_oK_d = 112,800$$

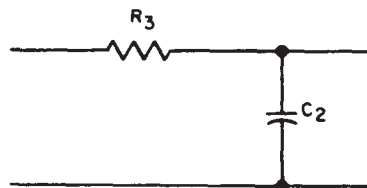
As shown in Fig. 20(a), for any second-order system, the loop natural frequency,  $\omega_n$  is:

$$\omega_n = (K/\tau)^{0.5}$$

where  $\tau$  is the integrating time constant of the loop filter. For the simple lag filter of Fig. 20(a),  $\tau_1 = R_3C_2$ .

Beyond this point, assumptions or specifications are needed with respect to the design requirements. One may optimize for noise, jitter, sweep rate, pull-in time, etc., depending on the application. For general and wide-ranging requirements, values for the loop-3dB bandwidth,  $\omega_{3dB}$ , and loop natural frequency can be assumed. Another choice is to look at the relation of noise bandwidth to damping factor,  $\zeta$ . If settling time is important, examine the phase error and damping factor as a function of  $\omega_{nt}$  ( $t = \text{time}$ ) where, for the settling time to be 90% complete, the value of  $\omega_n$  is given by the required settling time. Quoting from Gardner (and others see bibliography), for a phase error due to a step in delta phase,  $\omega_{nt}$  should be 4 for a damping factor of 0.5.

The simple lag filter has a limited range of capability but it can be effective in noncritical applications. The  $R_3C_2$  time constant can be chosen by trial and error or by thumb rule as the reciprocal of 1.5 to 3 times the frequency. This



(A)

$$F_1(s) = 1/(s\tau_1 + 1)$$

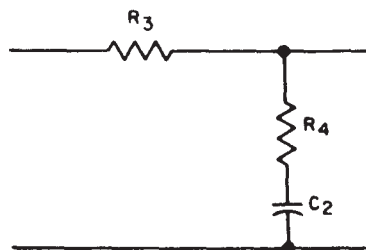
$$\tau_1 = R_3C_2$$

$$H_1(s) = (\omega_n^2 / (s^2 + 2\zeta\omega_n + \omega_n^2))$$

$$\omega_n = (K_oK_d/\tau_1)^{0.5}$$

$$\zeta = (1/4\tau_1K_oK_d)^{0.5}$$

92CS-43170



(B)

$$F_2(s) = (s\tau_2 + 1) / (s(\tau_1 + \tau_2) + 1)$$

$$\tau_1 = R_3C_2$$

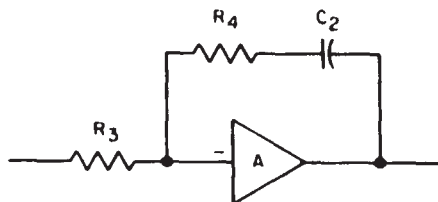
$$\tau_2 = R_4C_2$$

$$H_2(s) = [s(2\zeta\omega_n - \omega_n^2) + \omega_n] / (s^2 + 2\zeta\omega_n + \omega_n^2)$$

$$\omega_n = (K_oK_d/(\tau_1 + \tau_2))^{0.5}$$

$$\zeta = (\omega_n/2)[\tau_2 + (1/K_oK_d)]$$

92CS-43171



(C)

For large values of A (amp gain):

$$F_3(s) = -(s\tau_2 + 1) / s\tau_1$$

$$\tau_1 = R_3C_2 \quad \tau_2 = R_4C_2$$

$$H_3(s) = (2\zeta\omega_n s + \omega_n^2) / (s^2 + 2\zeta\omega_n s + \omega_n^2)$$

$$\omega_n = (K_oK_d/\tau_1)^{0.5}$$

$$\zeta = \omega_n\tau_2/2$$

92CS-43172

Fig. 20- Forms of low-pass filters (LPF) and associated loop equations.

approach favors lower damping factors to achieve low jitter with compromises for pull-in range and time. Two filters were tried for this example, as follows:

$\tau_1$	$R_3$	$C_2$	pull-in	$\omega_n$ (calc.)	$\zeta$ (calc.)
2.5 ms	51 k $\Omega$	0.047 $\mu$ F	$\pm 1$ kHz	6717 rad/s	0.032
25 $\mu$ s	51 k $\Omega$	487 pF	$\pm 4.25$ kHz	67.17 krad/s	0.32

When filters are designed by choosing an  $\omega_{3dB}/\omega_n$  ratio, the simple lag filter has a solution in terms of  $\zeta$  that is different from that of the lag-lead solution. In any case, the  $\omega_{3dB}$  solutions are derived by setting  $|H(j\omega)|^2 = 0.5$  and solving for  $\omega_{3dB}/\omega_n$ . However, experience is the best teacher, and the assumption of time-constant values, followed by the measuring and plotting of results, is an effective way to optimize values for those parameters important to an application.

## 2. Using PC2 With a Lag-Lead Filter

In this example, the lag-lead filter shown in Fig. 20(b) is used, and no offset-frequency requirement is specified. For the VCO section:

$$V_{CC} = 6 \text{ V}, f_{osc} = 1.2 \text{ MHz at } VCO_{in} = 4.5 \text{ V}$$

After following procedures similar to those described in the previous examples, the value of  $C_1$  is determined to be 100 picofarads, and  $R_1$  is found to be 62 kilohms. The VCO measurements are then:

$$f_{osc} = 1.16 \text{ MHz at } VCO_{in} = 4.5 \text{ V}$$

$$f_{osc} = 380 \text{ kHz at } VCO_{in} = 1.6 \text{ V}$$

and the following can be calculated:

$$K_o = V_{CC}/4\pi = 0.48 \text{ V/rad}$$

$$K_d = (1.2 - 0.38)\text{MHz} \times 2\pi/(4.5 - 1.16)\text{V} = 1.77\text{E6 rad/V}$$

$$K = K_o K_d = 0.85\text{E6}$$

The relation of the filter bandwidth, defined as  $\omega_1$ , may be used to establish the relation of  $\tau_1$  and  $\tau_2$  in the lag-lead filter. Then, defining the ratio of  $\omega_1$  to  $\omega_n$  provides a practical basis for comparing time constants to the active parameters of the loop. The solution of  $|f(j\omega)|^2 = 0.5$  yields:

$$\omega_1 = 1/(\tau_2^2 + 2\tau_1\tau_2 - \tau_1^2)^{0.5}$$

which may be used to calculate  $\tau_1$  and  $\tau_2$  after the  $\omega_1/\omega_n$  ratio is assumed. Then, using the equation of Fig. 20(b):

$$\omega_n = [K/(\tau_1 + \tau_2)]$$

filter-component values  $R_3$ ,  $R_4$ , and  $C_2$  can be derived as follows:

$$\text{Given: } \omega_1 = 1\% \text{ of } f_{min}, \omega_1/\omega_n = 1/8$$

$$\text{Calculate: } \tau_1 = 0.0346 \text{ ms}, \tau_2 = 0.0092 \text{ ms}$$

$$R_1 = 51 \text{ kilohms}, R_4 = 1.36 \text{ kilohms},$$

$$C_2 = 0.00068 \text{ microfarad}$$

Where jitter is the ratio of phase displacement to signal period, the following PLL results were obtained:

SIG <sub>in</sub> (kHz)	Jitter (ns)	Percent of Period
1200	< 28	2.4
790	< 20	1.6
380	50	1.9

## 3. Simple Low-Pass Filter Using PC2

This example uses the results of Example No. 1 and redefines the criteria for the loop:

$$\text{Given: } \omega_1 = 100 \text{ Hz}, \omega_1/\omega_n = 1/10$$

$$K_d \text{ is now } V_{CC}/2\pi = 6/2\pi = 0.955 \text{ V/rad}$$

Basing this example on measured data:

$$K_o = 51400 \text{ rad/V}$$

$$K = K_o \times K_d = 49095$$

Using  $\omega_n = (K/\tau_1)^{0.5}$  and the value of  $\omega_n$  from the given data gives:

$$\tau_1 = 1.24 \text{ ms}, R_3 = 51 \text{ kilohms}, C_2 = 0.024 \mu\text{F}$$

Measured results give 0.5 microsecond of jitter (1.4% of period) at 27.5 kilohertz.

## 4. Simple Low-Pass Filter Using PC2 With Divide-By-N

This example uses one of the examples given in the VCO measured-data section above:

$$V_{CC} = 6 \text{ V}$$

$$R_1 = 43 \text{ kilohms}, C_1 = 39 \text{ pF}$$

$$\text{For } K_o, f_{osc} \text{ meas. at } VCO_{in} = 3 \text{ V}$$

$$K_o = 6.12\text{E6 rad/V}$$

$$K_d \text{ is } 0.955 \text{ V/rad (from previous example)}$$

Using the HC4024 7-Stage Binary Ripple Counter for a divide-by-N of 128 and PC2 in a simple RC LPF, the loop frequency is 20 kilohertz and:

$$K = K_o(K_d/N) = 45660$$

If it is assumed that  $\omega_1$  is 1% of the loop frequency or  $\omega_1 = 200$  Hz, and that  $\omega_1/\omega_n = (1/8)$ , then  $\omega_n = (K/\tau_1)^{0.5}$  gives a time constant,  $\tau_1$ , of 451 milliseconds. Choosing  $R_3 = 51$  kilohms gives  $C_2 = 0.0088$  microfarad. The jitter measured during lock was less than 0.6 microsecond or 1.2 %.

A tabulation of results using the same VCO and divide-by-N ratio, where  $\omega_1$  is 1% of the 20-kHz loop (200 Hz) and  $\omega_1/\omega_n$  is varied, is shown in Table 1.

Table 1 - Results for Simple Low-Pass Filter Using PC2 with Divide-By-N

$\omega_1/\omega_n$	$\omega_n$ (calc.) (rad/s)	$\tau_1$ (calc.) (ms)	$R_3$ (calc.) (kilohms)	$C_2$ (calc.) ( $\mu$ F)	Jitter (meas.) ( $\mu$ s)	$\zeta$ (calc.) (d.f.*)
3	3774	3.206	51	0.0628	5	0.041
5	6290	1.154	51	0.0226	2	0.069
8	10064	0.451	51	0.0088	0.6	0.11
10	12580	0.288	5	0.0056	1.2	0.14

\*d.f. = damping factor



the range of pull-in remained typically the same for the 1-kilohertz loop. The pull-in measured 6 to 37 kilohertz.

#### Simple RC LPF Using Frequency Offset and PC2

To provide a comparison with loop example No. 4, a VCO example without the divide-by-N was developed using  $R_1 = 160$  kilohms,  $R_2 = 180$  kilohms and  $C_1 = 0.005$   $\mu$ F. The measured frequency for  $V_{CC} = 6$  V is:

VCO <sub>in</sub> (V)	f <sub>osc</sub> (meas) (kHz)
0	15.38 (offset)
1	17.85
1.75	20
3	22.78

Table II - Results for Simple RC LPF Using Frequency Offset and PC2

$\omega_l/\omega_n$	$\omega_n$ (calc.) (rad/s)	$\tau_1$ (calc.) (ms)	$R_3$ (calc.) (kilohm)	$C_2$ (calc.) ( $\mu$ F)	Jitter(meas.) ( $\mu$ s)	$\zeta$ (calc.)
3	3774	3.206	51	0.011	5.5	0.18
6.3	7952	1.154	51	0.0041	4	0.3
8	10064	0.451	51	0.00161	2	0.48
10	12580	0.288	51	0.001	0.6	0.6

$$K_o = 2\pi(22780 - 20000)/(3 - 1.75) = 13973 \text{ rad/V}$$

$$K_d \text{ is } 0.955 \text{ V/rad}$$

$$K = K_o K_d = 13344$$

Using  $\omega_l = 200$  Hz and  $\omega_l/\omega_n = 1/10$ , and solving as above gives the results of table II.

The pull-in is typically 18 to 33 kilohertz for this example. It should be noted that the damping factor,  $\zeta$ , is higher than in example No. 4. With offset, the loop-gain factor,  $K$ , is approximately 1/3 less.

#### DESIGN SUMMARY

There are several points to be made on the subject of LPF design. The examples shown in this Note are given as illustrations of HC/HCT4046A PLL capability. Indeed, the best recommendation for a general-purpose PLL would be to use an active filter. The gain factor,  $K$ , would then provide another degree of latitude in the many compromises of PLL design. The second best filter would be the lag-lead filter network design, where the added resistor provides a semi-independent control over the damping factor of the loop, a key requirement in tracking systems. The lag-lead, however, is an imitation of the active filter only for a limited range of component values. If the primary requirement is to phase-lock two frequencies synchronously together, and response time is not a major factor, the simple RC filter may be quite adequate for this purpose.

Because the filter design is not rigid, options exist to vary the design approach. Optimizing by trial and error should be considered in all cases. One should always be aware that textbook approaches are often developed for applications not identified or with limitations and assumptions not given. A few points that may help to clarify the assumptions made in the examples given in this Note are as follows:

1. Open-loop analysis has limited significance. The PLL is a system within itself, and nearly all technical material is presented in the form of a closed-loop analysis. The "bottom line" is that the filter must be designed with the entire loop in mind.
2. The HC/HCT4046A VCO gain factor,  $K_o$ , is dependent on the center frequency,  $f_o$ , and the offset frequency,  $f_{min}$ . That is,  $K_o$  is approximately  $(f_o - f_{min})/(V_{CC}/2)$ . If any of the VCO parameters such as  $R_1$ ,  $R_2$ , or  $C_1$  change, then  $K_o$  and the filter design requirements will change.

3. The use of a filter bandwidth of 1% of the signal or loop frequency may not achieve the desired results in all applications. Because no specific applications were defined in the above material, the 1% filter bandwidth,  $\omega_l$ , was chosen as a practical way to achieve simple phase-lock results, given that  $\omega_l/\omega_n$  is chosen for a practical range of component values. In any case, the designer should be aware of the common parameters used to describe the PLL performance, such as damping factor,  $\zeta$ ; loop natural frequency,  $\omega_n$ ; noise bandwidth, BL (or 2BL); and the loop gain,  $K = K_o K_d$ .

4. The damping factor can be used as a starting point for design assumptions. For some applications, this approach could be a better one than choosing bandwidths. The system response, however, must take into account both the loop natural frequency and the damping factor.

5. As noted in the VCO description, the linear range of the HC/HCT4046A extends from 1 volt to approximately  $V_{CC} - 1$  volt. Operation of the VCO<sub>in</sub> at or near the  $V_{CC}$  level is not recommended because the linear range of the internal differential amplifiers (CMA circuit) is exceeded. When this level of operation occurs, the  $K_o$  of the VCO increases rapidly and may cause loop instability. The application of active op-amp filter circuits using such devices as the CA5470 can limit the maximum positive voltage swing to approximately the correct level while operating from the same  $V_{CC}$  supply as the HC/HCT4046A.

The designer should apply high-speed application-circuit techniques when using High-Speed CMOS PLL devices; the switching speed can produce higher harmonic components. Good rf bypassing techniques with good filtering are recommended in the design of the power-supply distribution to minimize any potential EMI problems.



**BIBLIOGRAPHY AND REFERENCES**

1. **Phase-Lock Techniques**, F.M.Gardner, John Wiley & Sons, NY
2. **Frequency Synthesis**, V.F.Krupa, John Wiley & Sons, NY
3. **Engineering Electronics**, J.D.Ryder, McGraw Hill, NY
4. "Color-Carrier Reference Phase Synchronization Accuracy in NTSC Color Television," D.Richman, **Proceedings IRE**, 42, 106-33, 1954
5. "Miniaturized RC Filter Using Phase-Locked Loop," G.S.Moschytz, **Bell System Tech. Journal**, page 829, 1965

**ACKNOWLEDGMENTS**

Contributions to this Application Note were provided by J. Nadolski (device characteristics) and C. Lee (PLL filter examples).